RSC Advances

ROYAL SOCIETY OF CHEMISTRY

www.rsc.org/advances

Cite this: DOI: 10.1039/c0xx00000x

www.rsc.org/ xxxxxx

COMMUNICATION

Seed-induced synthesis of hierarchical ZSM-5 nanosheets in the presence of hexadecyl trimethyl ammonium bromide

Min Liu, Junhui Li, Wenzhi Jia, Mengjiao Qin, Yanan Wang, Kai Tong, Chen Huanhui and Zhirong Zhu*

Received (in XXX, XXX) Xth XXXXXXXXX 20XX, Accepted Xth XXXXXXXXX 20XX
DOI: 10.1039/b000000x

Hierarchical ZSM-5 nanosheets with intracrystal mesopores and honeycomb morphology have been synthesised by seed-inducing via a hydrothermal route in the presence of hexadecyl trimethyl ammonium bromide (CTAB) as the second template.

Zeolites with shape selectivity and molecular sieve effect due to their uniform micropores, have been extensively used as heterogeneous catalysts in industrial applications. However, their relatively small individual micropores limit the diffusion rate of reagents and reaction products, which decreases catalytic efficiency, especially for reactions involving macromolecules.[1-4] To solve this problem, researches have proposed several approaches (such as nanosized zeolites and ordered mesoporous materials).[5-8] Hierarchical zeolites combined features of microporous materials with improved transport rate are considered the best strategy and have stimulated much research.[9-11] Generally, a second pore system in zeolite crystals can be introduced via post-treatment (*e.g.* steaming, base or acid leaching) of the synthesised zeolites or introducing templates (including soft templating method and hard templating method) during the zeolites crystallisation.[12-15] Among these methods, soft templating method is the preferred approach because it has good compatibility with zeolites precursors and offers the opportunity to generate controllable mesopores based on the molecular size. Recently, MFI zeolite nanosheets were prepared by using designed bifunctional surfactant ($C_{22}H_{45}$-$N^+(CH_3)_2$-C_6H_{12}-$N^+(CH_3)_2$-C_6H_{13}) as template,[4,16,17] however, the synthesis process of this template is very complex that the synthesise of MFI zeolite nanosheets becomes costly. Hierarchical ZSM-5 zeolite with house-of-card-like was synthesised with the assistance of N-Methyl-2-pyrrolidone (NMP).[18] Although NMP is one of common inexpensive solvents, it has environmental issues. Traditional surfactants CTAB as soft templates are of great interest because of low cost and little environmental impact. CTAB, which although has a competition between self-assemble and zeolites crystallization, have been used to synthesise hierarchical ZSM-5 zeolites by kinetic control over zeolite seed formation,[19,20] or with the assist of modified organosilane (*e.g.* sulfonic acid-ended organosilane or carboxyl-ended organosilane).[21,22] Nevertheless, to the best of our knowledge, using CTAB as soft template, most hierarchical ZSM-5 zeolites reported are sphere-like,[19-22] which show poor crystal morphology and hinder its further industrial applications because of difficulties in reactants and productions diffusion.[23,24] Herein, by seed-inducing, the hierarchical ZSM-5 (Hi-ZSM-5) nanosheets with intracrystal mesopores and honeycomb morphology were green synthesised via hydrothermal route in the presence of CTAB as the second template. For comparison, conventional ZSM-5 (C-ZSM-5) zeolite was prepared with the same procedure except for the absence of CTAB.

The scanning electron microscope (SEM) images (Fig. 1 (a) and (b)) clearly show the morphology of Hi-ZSM-5 zeolites in low and high magnifications, respectively. Significantly different from rectangular C-ZSM-5 zeolites (see Fig. S1 (a) and (b), ESI†), Hi-ZSM-5 zeolite was a honeycomb-like particle with particle size of 2-4 μm, which composed of decussate zeolite slice units. The zeolites mainly grew in three dimensions that the mesopores and macropores were formed between adjacent slices. The

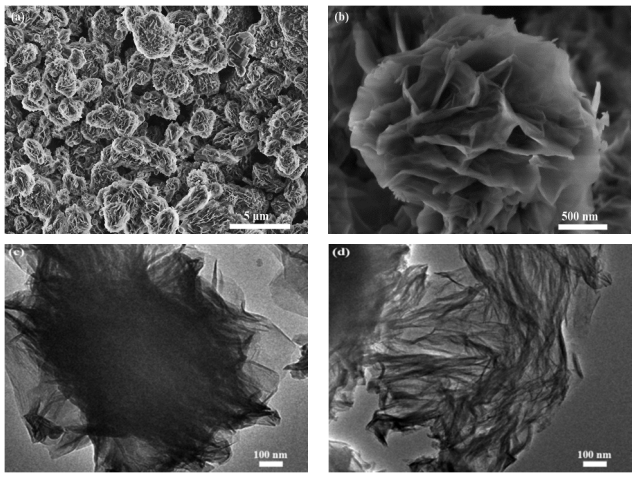

Fig. 1 SEM images for Hi-ZSM-5 samples (a) low magnification and (b) high magnification; HR-TEM images for Hi-ZSM-5 samples (c) and (d).

Department of Chemistry, Tongji University, Shanghai 200092, China. Fax: +86-21-65981097; Tel: +86-21-65982563; E-mail: zhuzhirong@tongji.edu.cn

† Electronic Supplementary Information (ESI) available: Detailed experimental procedures, SEM and TEM images of Hi-ZSM-5, ZSM-5 seeds and C-ZSM-5, nitrogen adsorption/desorption isotherms and BJH pore size distribution curves of Hi-ZSM-5, SEM images and FT-IR, XRD spectras of subnanocrystals, detailed product conversion, yield, selectivity and stability data See DOI: 10.1039/b000000x/

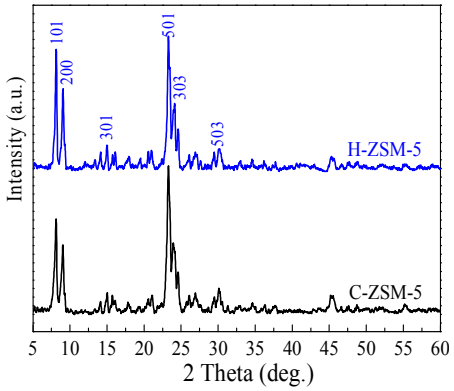

Fig. 2 XRD patterns of Hi-ZSM-5 and C-ZSM-5

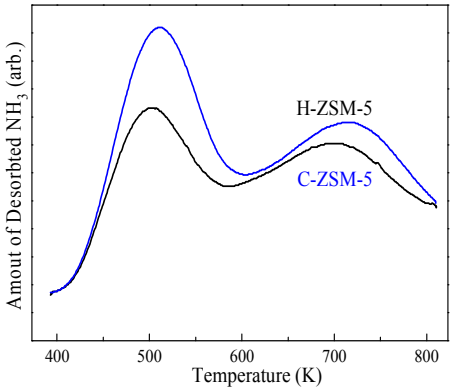

Fig. 3 NH_3-TPD spectra of Hi-ZSM-5 and C-ZSM-5

hexagonal zeolites in the top-right were ZSM-5 seeds which had not dissolved completely (see Fig. S2 (a) and (b), ESI†). Additionally, there were very few small amorphous silica particles on the surface of Hi-ZSM-5 zeolites. This resulted from the competition of CTAB and structure-directing agents (tetrapropyl ammonium bromide (TPABr)) with zeolite precursors, which could not disappear throughly. High-resolution transmission electron microscopy (HR-TEM) images show that Hi-ZSM-5 zeolites (Fig. 1 (c) and (d)) have only slices, no nucleus was found in the inner of zeolites which is in good accordance with the section SEM images (see Fig. S3 (a) and (b), ESI†). Moreover, no defects can be observed in different shade HR-TEM images (see Fig. 1 and Fig. S4, ESI†), suggesting that the zeolites have a high crystallinity.

Fig. 2(a) shows the X-ray diffraction (XRD) patterns of Hi-ZSM-5 and C-ZSM-5. Both of them gave a typical pattern of MFI structure (2θ at around 8.0°, 9.0°, 14.8°, 22.9°, 24.0° and 29.8° corresponding to the major peaks of 101, 200, 301, 501, 303 and 503 crystal surfaces). Compared with C-ZSM-5, the relative crystallinity of Hi-ZSM-5 was 96%. This was estimated by comparing the peaks between 2θ = 22.5° and 25.0°. Meanwhile, XRD patterns of Hi-ZSM-5 confirm that Hi-ZSM-5 was highly crystallized MFI nanosheets, contrasting to the characteristic of a crystalline MFI reported by Ryoo et al[4]. This may be due to the addition of TPABr and ZSM-5 seeds that enhanced the directing process, in good accordance with Liu report[17]. The N_2 adsorption-desorption isotherms of Hi-ZSM-5 and the textural parameters of Hi-ZSM-5 and C-ZSM-5 samples are shown in Fig. S5, ESI† and Table S1, ESI†. The steep increase occurring in adsorption near $P/P_0 = 0$ was due to the filling of zeolite micropores. There was a hysteresis loop at P/P_0 of 0.4-0.9 which indicated the presence of mesoporous structure. And the hysteresis loop is a type-H3 isotherm, suggesting that the mesopores were almost slit-like.[25] In order to avoid the misinterpretation of uniform mesopores of 4 nm, the adsorption data were used to calculate the pore size distribution by Barrett-Joyner-Halenda (BJH) method[26] (see Fig. S5, ESI† inset) and the pore size mainly distributed around 3-7 nm. Furthermore, although the total specific surface area of Hi-ZSM-5 estimated by the BET method was close to that of C-ZSM-5 (397 m^2/g and 381 m^2/g, respectively), Hi-ZSM-5 had much larger mesopore volumes than that of C-ZSM-5 (0.17 cm^3/g and 0.04 cm^3/g, respectively), which was owning to the presence of mesopores (see Table S1, ESI†).

In a typical synthesis, H-form ZSM-5 zeolites were obtained by ion- exchange with NH_4NO_3 and subsequent calcination at 813 K. Fig. 3 shows the temperature-programmed desorption of ammonia (NH_3-TPD) curve of Hi-ZSM-5 and C-ZSM-5 samples and both of them had similar-shaped curves. The peak at 393-573 K attributed to desorption of NH_3 adsorbed on weak acidic sites, while the peak at 573-773 K assigned to strong acidic sites. Interestingly, the concentration of surface acid sites and the weak acid sites fraction of Hi-ZSM-5 were higher than that of C-ZSM-5, based on the area integral of entire NH_3-TPD curves. This was mainly due to there were more accessible acid sites in Hi-ZSM-5 because of layer structure, while C-ZSM-5 grains may aggregated and a portion of acid sites could not be accessed. Considering the above results and discussions, it indicated that Hi-ZSM-5 may show better catalytic performances in alkylation toluene with methanol which needs higher mild acid concentration, compared with C-ZSM-5.

The prepared samples and two kind of commercial ZSM-5 zeolite (Si/Al=45, Si/Al=50) were tested by the alkylation of toluene with methanol, and C-ZSM-5 had similar catalytic performances as commercial ZSM-5 (Si/Al=50) did. Notably, Hi-ZSM-5 showed a higher conversion than C-ZSM-5 (48.2% and 41.3% respectively, see Table S2, ESI†) because of its higher concentration of surface acid sites coupled with layer structure.[27] Notably, while Hi-ZSM-5 showed a similar toluene conversion as conventional ZSM-5 (Si/Al=45) (48.2% and 44.8% respectively, see Table S2, ESI†) because of the similar acidity (see Table S3, ESI†), it had a higher conversion than that of C-ZSM-5 (41.3%) owing to its higher concentration of surface acid sites coupled with layer structure (see Table S3, ESI†).[27] Moreover, xylene selectivity of Hi-ZSM-5 was 81.7%, which was 16.3% and 17.9% higher than those of C-ZSM-5 and commercial ZSM-5 (Si/Al=50), respectively (see Table S2, ESI†). This was mainly because of a relatively higher concentration of xylene exists in the inner of C-ZSM-5 commercial ZSM-5 crystals due to the limitation of diffusion, which easily lead to the formation of trimethylbenzene. On the contrary, Hi-ZSM-5 zeolites, with a shorter diffusion path, xylene product was easier to come to the gas phase and could restraint the successive alkylation of xylene .[23,24] In addition, the benzene selectivity of Hi-ZSM-5 (7.9%) was much lower than those of C-ZSM-5 and commercial ZSM-5 (Si/Al=45) (28.4% and 16.3% respectively, see Table S2, ESI†). This result from that higher strong acid fraction of C-ZSM-5 may accelerate the process of toluene disproportionation, leading to high content of benzene, while commercial ZSM-5 (Si/Al=45) had a lower alkylation and diffusion rate. Also, Hi-ZSM-5 showed a longer catalytic lifetime than that of C-ZSM-5 (see Fig. S9, ESI†). This was mainly due to Hi-ZSM-5 can

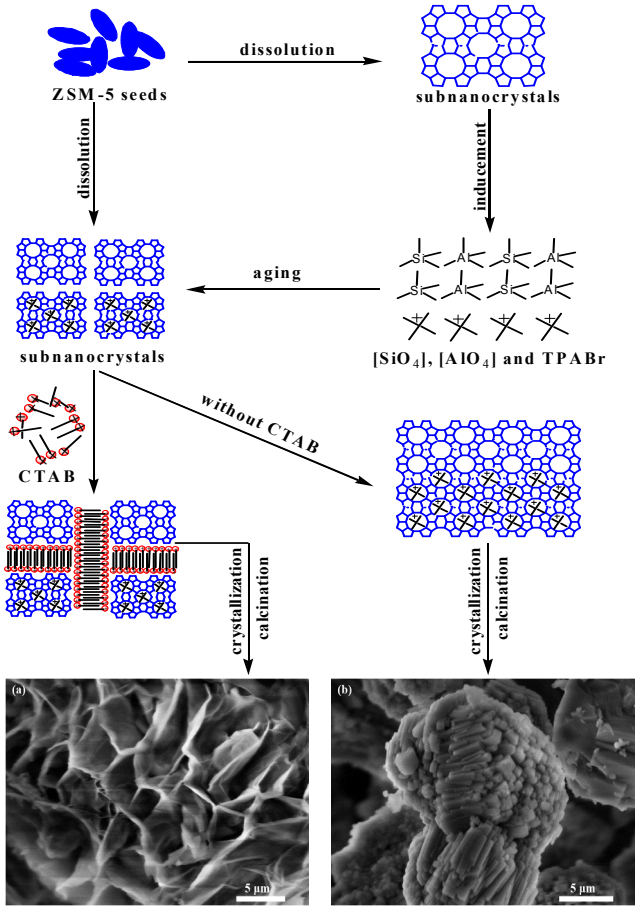

Fig. 4 Proposed possible mechanism for the self-assembly between subnanocrystals and CTAB under hydrothermal condition, (a) Hi-ZSM-5, (b) C-ZSM-5.

integrate the features of mesoporous and layer crystal structure, which was propitious to transport coke precursors out of the zeolites, thus having a low carbon deposition rate and long catalytic lifetime. Therefore, with the hierarchical structure, Hi-ZSM-5 show the better catalytic performance than C-ZSM-5, which was attributed to hierarchies provided higher acid sites concentration and boosted the efficiency of benzene alkylation and diffusion rate. This was in good agreement with previous reports.[4,17,18,26]

The approach of seed-induced synthesis of MFI zeolites havebeen reported by many literatures.[28,29] But the synthesis mechanism is still elusive. Based on the previous study,[19,30] the possible formation mechanism of Hi-ZSM-5 was proposed in this paper (Fig. 4). In present work, we suggested that the ZSM-5 seeds may be dissolved into subnanocrystals which have the primary structure of MFI zeolites at first (see Fig S6, S7and S8 ESI†). Then these subnanocrystals induced the primary units [SiO_4] and [AlO_4] into a large amount of subnanocrystals with the help of the structure-directing agent TPABr by the proceeding of aging. During this period, the dissolution and inducement take place simultaneously. When the mesoporogens CTAB added into the mixture, these subnanocrystals interacted with CTAB and form Hi-ZSM-5 zeolites at elevated temperature by hydrothermal treatment. While the competition between CTAB self-assembly and TPABr templating could be decreased greatly due to the formation of subnanocrystals which could easily to crystallize. On the other hand, without CTAB added into the mixture, TPABr bind to the surface of subnanocrystals in crystallization and could not lead to formation of mesopores.

In summary, Hi-ZSM-5 zeolites with intracrystal mesopores and honeycomb morphology were synthesised by seed-induced assemble the nanocrystal. Catalytic test indicated that Hi-ZSM-5 zeolites show higher activity compared to C-ZSM-5 zeolites. This difference is due to the presence of mesopores, which accelerate the diffusion rate and enhance the catalytic efficiency. This may provide a novel way to improve performance in the industrial application of zeolites. Furthermore, by using this method, different hierarchical zeolites (such as mordenite, zeolite X and Y) may be synthesised as well.

This work was financially supported by National Natural Science Foundation of China (Grant No.20873091 and 51174277) and China National Petroleum Corporation Innovation Research Funds (Grant No.2012D-5006-0505). The authors would like to thank Dr van Bokhoven and an anonymous referee for their constructive comments which helped us to improve the manuscript.

Notes and references

1 A. Corma, *Chem. Rev.*, 1997, 97, 2373.
2 M. E. Davis, *Nature,* 2002, 417, 813.
3 C. S. Cundy and P. A. Cox, *Chem. Rev.*, 2003, 103, 663.
4 M. Choi, K. Na, J. Kim, Y. Sakamoto, O. Terasaki and R. Ryoo, *Nature*, 2009, 461,2 46.
5 C. T. Kresge, M. E. Leonowicz, W. J. Roth, J. C. Vartuli and J. S. Beck, *Nature*, 1992, 359, 710.
6 X. Bu, P. Feng and G. D. Stucky, *Science*, 1997, 278, 2080.
7 Y. Liu, W. Zhang and T. J. Pinnavaia, *Angew. Chem. Int. Ed.*, 2001, 40, 1255.
8 G. T. Vuong and D. Trong On, *J. Am. Chem. Soc.*, 2007, 129, 3810.
9 Z. Yang, Y. Xia and R. Mokaya, *Adv. Mater.*, 2004, 16, 727.
10 M. Choi, H. S. Cho, R. Srivastava, C. Venkatesan, D. Choi and R. Ryoo, *Nat. Mater.*, 2006, 5, 718.
11 J. Pérez-Ramírez, C. H. Christensen, K. Egeblad, C. H. Christensen and J. C. Groen, *Chem. Soc. Rev.*, 2008, 37, 2530.
12 J. C. Groen, T. Bach, U. Ziese, A. M. Paulaime-van Donk, K. P. de Jong, J. A. Moulijn and J. Pérez-Ramírez, *J. Am. Chem. Soc.*, 2005, 127, 10792.
13 Y. Zhou and M. Antonietti, *Chem. Commun.*, 2003, 20, 2564.
14 H. Wang and T. J. Pinnavaia, *Angew. Chem. Int. Ed.*, 2006, 45, 7603.
15 K. Na, C. Jo, J. Kim, K. Cho, J. Jung, Y. Seo, R. J. Messinger, B.F. Chmelka and R. Ryoo, *Science*, 2011, 333, 328.
16 K. Na, M. Choi, W. Park, Y. Sakamoto, O. Terasaki and R. Ryoo. *J. Am. Chem. Soc.* 2010, 132, 4169.
17 E. Laleh, Y. Wu, G. Zhu, C.C. Chang, W. Fan, T. Pham, R. F. Lobo and D. Liu. *Chem. Mater.*, 2014, 26, 1345.
18 L. Liu, H. Wang, R. Wang, C. Sun, S. Zeng, S. Jiang, D. Zhang, L. Zhu, and Z. Zhang. *RSC Adv.*, 2014, 4, 21301.
19 Y. Zhu, Z. Hua, J. Zhou, L. Wang, J. Zhao, Y. Gong, W. Wu, M. Ruan and J. Shi, *Chem. Eur. J.*, 2011, 17, 14618.
20 Y. Zhu, Z. Hua, Y. Song, W. Wu, X. Zhou, J. Zhou and J. Shi, *J. Catal.*, 2013, 299, 20.
21 H. Jin, M. Bismillah Ansari and S.-E. Park, *Chem. Commun.*, 2011, 47, 7482
22 Y. Zhang, K. Zhu, X. Duan, P. Li, X, Zhou and W. Yuan, *RSC Adv.*, 2014, 4, 14471.
23 C. H. Christensen, K. Johannsen, I. Schmidt and C. H. Christensen, *J. Am. Chem. Soc.*, 2003, 125, 13370.
24 M. S. Holm, E. Taarning, K. Egeblad and C. H. Christensen, *Cata.*

Today, 2011, 168, 3.
25 G. Leofanti, M. Padovan, G. Tozzola and B. Venturelli, *Cata. Today*, 1998, 41, 207.
26 J. C. Groen, L. A. A. Peffer and J. Pérez-Ramírez, *Micropor. Mesopor. Mat.*, 2003, 60, 1.
27 X. Zhang, D. Liu, D. Xu, S. Asahina, K. A. Cychosz,K. V. Agrawal, Y. Al Wahedi, A. Bhan, S. Al Hashimi,O. Terasaki, M. Thommes and M. Tsapatsis, *Science*, 2012, 336, 1684
28 N. Ren, Z. Yang, X. Lv, J. Shi, Y. Zhang, and Y. Tang, Micropor. Mesopor. Mat., 2010, 131,103.
29 G. Majano, A. Darwiche, S. Mintova and V. Valtchev, *Ind. Eng. Chem. Res.*, 2009, 48, 7084.
30 C.S. Cundy, P.A. Cox, *Micropor. Mesopor. Mat.*, 2005, 82, 1.